Journal of Mines, Metals and Fuels, *73(11): 3387-3399; 2025. DOI: 10.18311/jmmf/2025/49968*

Print ISSN : 0022-2755

Journal of Mines, Metals and Fuels

Contents available at: *www.informaticsjournals.co.in/index.php/jmmf*

Effects of Temperature-Dependent Viscosity and Chemical Reaction on MHD Hybrid Carbon Nano Dissipative Fluid Flow with Heat Source

K. Fatima[1] and J. L. Rama Prasad[2*]

[1]Department of Mathematics, Krishna University, Machilipatnam - 521001, Andhra Pradesh, India
[2]Department of Mathematics, P. B. Siddhartha College of Arts and Science, Vijayawada - 520010, Andhra Pradesh, India; jlrprasad@gmail.com

Abstract

This study addresses the effects of temperature-dependent variable viscosity and thermal conductivity in an MHD hybrid nanofluid using Single-Walled and Multi-Walled Carbon Nanotubes (SWCNTs and MWCNTs) with water as the base fluid. Slip effects via a permeable sliding plate and Joule heating are considered. The governing equations are transformed into Ordinary Differential Equations (ODEs) using similarity transformations, which are then solved using MATLAB's bvp4c tool. Results are presented in tabular form and through graphical representations, showing the impact of non-dimensional parameters on hybrid nanofluid flow. The hybrid nanofluid, consisting of SWCNTs and MWCNTs in water, effectively describes the flow behaviour and heat transfer by accounting for temperature-dependent changes in viscosity, thermal conductivity and slip boundary conditions. The influence of variable viscosity on the skin friction coefficient in boundary layer flow over a moving flat plate is examined. Additionally, the impact of temperature-dependent thermal conductivity on the Nusselt number is analysed, demonstrating improved heat transfer efficiency through modifications in the thermal boundary layer properties. The investigation of slip boundary conditions in hybrid nanofluids aims to enhance velocities near the wall, reduce frictional resistance and optimise heat transfer rates. Viscous dissipation in the hybrid nanofluid significantly affects its thermal and flow properties, thereby influencing temperature distribution and heat transfer efficiency. The combined effects of variable viscosity and thermal conductivity in SWCNT-MWCNT hybrid nanofluids with water as the base fluid can enhance heat transfer, flow regulation and thermal stability, with potential applications in the mining, metal processing and fuel industries.

Major Findings: *The study investigates the effects of temperature-dependent viscosity and thermal conductivity to better reflect realistic fluid behaviour. Numerical results demonstrate that these variable fluid properties significantly influence the velocity, temperature and concentration profiles. The findings provide valuable insights for engineering applications involving thermal management, flow control and the design of systems requiring enhanced thermal stability.*

Keywords: *Hybrid Nanofluid, Moving Plate, Slip Velocity, Variable Thermal Conductivity, Variable Viscosity, Viscous Dissipation*

1.0 Introduction

Heat management technologies have advanced with hybrid nanofluids, which contain several nanoparticles in a base fluid. Unique nanoparticle properties promote thermal conductivity, heat transmission and fluid stability. These are used in more industrial processes when combined with heat sources, chemical reactions and thermal radiation.

Carbon Nanotubes (CNT) are hexagonal carbon atoms in cylindrical shape, existing in Single-walled and

**Author for correspondence*

multi-walled carbon nanotubes (CNTs) forms, SWCNT or MWCNT combined with water and nanoparticles like metal oxides and graphene form a water-based hybrid nanofluid with good thermal and functional characteristics. By enhancing heat transmission, SWCNT/MWCNT hybrid nanofluids increase condenser and evaporator performance and minimise refrigeration energy usage. Radiation resistance and temperature stability make SWCNT/MWCNT-based nanofluids advanced coolants that increase nuclear reactor safety and efficiency. Due to enhanced optical absorption, water-based hybrid nanofluids with CNTs optimise the direct absorption of solar collector solar energy.

CNT-hybrid nanofluids cool engines faster and save gas. It simplifies distillery and power plant phase adjustments. CNT-based hybrid nanofluids comprising biocompatible water and medicines are being investigated for targeted drug delivery, MRI/CT scanner cooling. SWCNT-MWCNT water improves membrane distillation and freshwater generation and improves reverse osmosis and hybrid nanofluid Modified Energy Distribution (MED) heat transfer. Hybrid nanofluids with CNTs cool space and aviation electronics and propulsion. Environmental impact is reduced by CNT-based fluid recycling.

Understanding how temperature influences the physical properties of materials is crucial in multiple scientific and industrial applications. Two essential properties that significantly depend on temperature are viscosity and thermal conductivity. The relationship between these properties and temperature is of theoretical significance as well as practical applications, ranging from engineering to food science.

Variable viscosity refers to the property of a fluid whereby its viscosity changes in response to altering conditions such as shear rate, temperature or pressure. This characteristic helps distinguish Newtonian fluids, which have constant viscosity regardless of shear rate, from non-Newtonian fluids, which can increase or decrease in viscosity under different conditions. The important attribute of temperature-dependent thermal conductivity measures how materials' thermal conductivity changes with temperature. This phenomenon is important in heat transfer, material science and engineering because materials' heat conductivity varies with temperature.

Shahirah *et al.*,[1] explored mixed convection flow using a hybrid nanofluid across a permeable shrinking surface at the stagnation-point area, considering second-order velocity slip changing viscosity. Himanshu Chaudhary *et al.*,[2] studied Magnetohydrodynamics (MHD) slip flow convective heat transfer generated by a permeable sliding plate with changing viscosity and thermal conductivity. Lorenzo Fusi and Rebecca Tozzi[3] studied piezoviscous fluid boundary layer flow over a stretched wedge and pressure-dependent viscosity, also considering second-order velocity slip, chemical processes and other fluid properties. S. Manjunatha *et al.*,[4] studied how modifying fluid parameters, such as viscosity, natural convection and Lorentz force, might improve heat transmission. They focused on free convection using suspended hybrid nanofluids. A moving wedge was used to study SWCNT–MWCNT/water hybrid nanofluid flow, heat transfer by Shafiq Ahmad *et al*[5]. In conjunction with the modified Buongiorno model, Sohaib Abdal *et al.*,[6] stressed the importance of non-uniform viscosity from rotating flow around a sphere with homogeneous Ag and CuO nanoparticles in water. Dharmaiah G *et al.*,[7] focused on free convective heat, mass transfer properties of magneto flow through a moving inclined plate under an aligned magnetic field. Vedavathi N *et al.*,[8] conducted a numerical investigation to review the entropy study of MHD convection nanofluid flow from an inclined surface.

Zeeshan *et al.*,[9] studied steady-state electrically conducting immiscible fluids between two parallel vertical plates in two sections with engine-oil- and water-based CNTs in porous media. Saqib Murtaza *et al.*,[10] studied unsteady hybrid Nanofluid (NF) flow using ($CoFe_2O_4$)-(Copper) nanoparticles, using natural convection from an expanding porous surface. Hanifa Hanif *et al.*,[11] examined entropy formation in (Fe_3O_4–Copper)/water hybrid nanofluid through a porous vertical cone with variable wall temperature. Nur Adilah Liyana Aladdin *et al.*,[12] showed hybrid carbon nanotube MHD flow over a permeable sliding plate, accounting for Joule heating, slip velocity. Flow, heat transfer from water-functionalized CNTs over a static/moving wedge with viscosity to assess their influence on thermofluid performance was quantitatively explored by Waqar Khan *et al*[13]. Hemanta Konwar[14] conducted a research to examine the MHD flow of incompressible viscous fluid across a continuously moving nonlinear sheet with temperature-dependent fluid parameters. Lakshmi BN *et al.*,[15] studied impact of magnetohydrodynamics and viscous dissipation effects of Fe_3O_4–$CoFe_2O_4$–H_2O across permeable sheet, incorporating the influence of Darcy–Forchheimer

consequences. Shankar Goud B. and G. Dharmaia[16] evaluated the behaviour of a gradually stretched sheet by analysing flow, heat transfer in the boundary layer, as well as investigating activation energy and Joule heating at the melting surface.

Animasaun Isaac Lare[17] investigated the viscosity, thermal conductivity in steady incompressible laminar free convective MHD non-Newtonian Casson fluid flow over a thermally stratified extending surface. N. Bhaskar Reddy *et al.*,[18] examined the 2D nanofluid with copper nanoparticles over a stretched sheet, considering convective boundary conditions, partial velocity slip. Bhose Ganga *et al.*,[19] investigated the convective 3D MHD Casson fluid through an unstable, stretched, permeable sheet with variable thermal conductivity. Sreenivasulu *et al.*,[20] studied MHD flow around a thermally stratified cylinder under stretching conditions, incorporating a heat source or sink with variable thermal conductivity. Hamza *et al.*,[21] synthesised research on hybrid nanofluid viscosity, including particle size and concentration, pH value, morphology and analysed viscosity effects. Taghreed H. Alarabi and A. Mahdy[22] introduced the boundary layer analysis for steady state free convection non-Newtonian micropolar fluid through an isothermal vertical permeable cone under the impact of variable thermal conductivity and thermophoretic force. Vivek Kumar Sharma and Aisha Rafi[23] examined the flow of viscous incompressible fluid in a variable free stream approaching the stagnation point on a non-conducting stretched sheet. Vijendra Singh and Shweta Agarwal[24] explored Maxwell fluid flow, heat transfer across stretched porous material with varying thermal conductivity.

This study presents a formulation of a mathematical flow model, incorporating temperature-dependent fluid properties, together with velocity slip boundary conditions. The governing equations comprise three essential equations: continuity, momentum and energy. The influences of MHD and Joule heating are included in the momentum and energy equations, respectively. Similarity transformation is employed to convert PDEs into ODEs. The BVP4c MATLAB function is utilised for numerical computation and graph plotting for analysis.

2.0 Mathematical Modelling

Initially, consider a 2D steady boundary layer of hybrid carbon nanotube slip flow through a permeable moving plate with the effects of MHD, Joule heating. Figure 1 illustrates that fluid flow is occupied in the region between the x and y axes (i.e., $x, y \geq 0$). This physical model relies on a few assumptions:

(i) The x-axis is parallel to the plate, while the y-axis is normal to it.

(ii) The parameter for a moving plate is λ. Here > 0 when the plate moves away from the origin, and $\lambda <$ 0 when it moves towards the origin.

(iii) The velocity slip effect (L) modifies the surface velocity boundary, permitting partial fluid adhesion.

(iv) Assuming T_w, C_w represents the plate temperature and concentration, while T_∞, C_∞ represent ambient fluid temperature and concentration

(v) The mass fluid velocity, $V_w = -\left(\frac{U\upsilon f}{2x}\right)^{1/2}$ S where $V_w > 0$ (suction) and $V_w < 0$ (injection). The impermeable surface is characterised when $V_w = 0$

(vi) SWCNT and MWCNT are chosen with concentrations of 1% - 3%. Nanoparticle shape is assumed to be uniform and spherical. Nanoparticles are considered to be in thermal equilibrium. The combination of nanoparticles is assumed to be stable.

In light of the above points, the governing equations consist of continuity, momentum and

Energy equations are written by using boundary layer approximations:

$$\frac{\partial u}{\partial x}+\frac{\partial v}{\partial y}=0 \tag{1}$$

$$u\frac{\partial u}{\partial x}+v\frac{\partial u}{\partial y}=\frac{1}{\rho_{hnf}}\frac{\partial}{\partial y}\left(\mu_{hnf}(T)\frac{\partial u}{\partial y}\right)- \frac{\sigma_{hnf}}{\rho_{hnf}}B_0^2(u-\mathrm{U})-\frac{\mu_{hnf}}{\rho_{hnf}}\left(\frac{u-U}{k^*}\right) \tag{2}$$

$$u\frac{\partial T}{\partial x}+v\frac{\partial T}{\partial y}=\frac{1}{(\rho C_p)_{hnf}}\frac{\partial}{\partial y}\left(K_{hnf}(T)\frac{\partial T}{\partial y}\right)+ \frac{\sigma_{hnf}}{(\rho C_p)_{hnf}}B_0^2(u-U)^2+\ldots \frac{\mu_{hnf}(T)}{(\rho C_p)_{hnf}}\left(\frac{\partial u}{\partial y}\right)^2+\frac{Q_0}{(\rho C_p)_{hnf}}(T-T_\infty) \tag{3}$$

$$u\frac{\partial C}{\partial x}+v\frac{\partial C}{\partial y}=D_m\frac{\partial^2 C}{\partial y^2}-k_r\left(C-C_\infty\right) \tag{4}$$

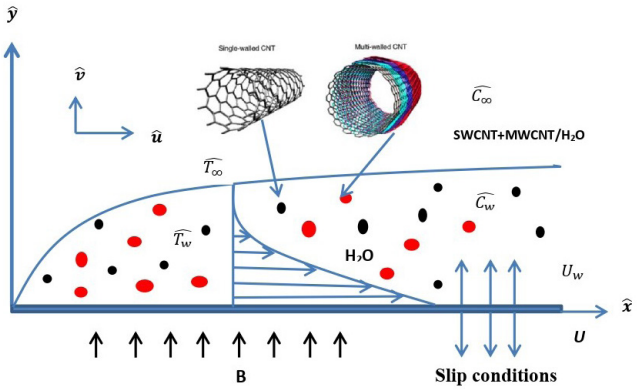


Figure 1. Physical model of the problem.

2.1 Boundary Conditions

$$\left.\begin{aligned} &u=\lambda U+L\frac{\partial u}{\partial y},\ v=V_w,\ T=T_w,\ C=C_w,\ at\ y=0\\ &u\to U,\ T\to T_\infty,\ C\to C_\infty,\ as\ y\to\infty \end{aligned}\right\} \tag{5}$$

Solving complex nonlinear partial differential equations is difficult and tedious. Thus, a similarity transformation was introduced to reduce the multiple independent variables in the PDE to an ODE with simple variables. Based on the boundary layer flow geometries and their boundary conditions, a stream function was used, ψ, where $u=\frac{\partial\psi}{\partial y}$ and $v=-\frac{\partial\psi}{\partial x}$.

Similarity transformations are given below as per Aladdin *et al*[12]:

Table 1. Thermophysical characteristics of nanoparticles and fluid Ahmed *et al*.,[5] and Alladin *et al*.,[12]

Physical Properties	Water(f)	SWCNT (φ_1)	MWCNT (φ_2)
Specific heat (C_p)	4179	425	796
Density (ρ)	997	2600	1600
Thermal Conductivity (k)	0.613	6600	3000
Electrical Conductivity (σ)	5.5×10^{-6}	1×10^{6}	1×10^{7}
Dynamic viscosity (μ)	1.002mPa-s (at 20°C)	-	-

Table 2. Thermophysical characteristics of Hybrid nanofluid Ahmed *et al*.,[5] and Alladin *et al*.,[12]

Properties	Nanofluid	Hybrid Nanofluid
Density	$\rho_{nf}=(1-\phi_1)\rho_f+\phi_1\rho_{s1}$	$\rho_{hnf}=(1-\phi_2)[(1-\phi_1)\rho_f+\phi_1\rho_{s1}]+\phi_2\rho_{s2}$
Heat Capacity	$(\rho Cp)_{nf}=(1-\phi_1)(\rho Cp)_f+\phi_1(\rho Cp)_{s1}$	$(\rho Cp)_{hnf}=(1-\phi_2)[(1-\phi_1)(\rho Cp)_f+\phi_1(\rho Cp)_{s1}]+\phi_2(\rho Cp)_{s2}$
Dynamic Viscosity	$\mu_{nf}=\frac{\mu_f}{(1-\varnothing_1)^{2.5}}$	$\mu_{hnf}=\frac{\mu_f}{(1-\varnothing_1)^{2.5}(1-\varnothing_2)^{2.5}}$
Thermal Conductivity (Hamilton Crosser model)	$k_{nf}=\frac{k_{s1}+(m-1)k_f-(m-1)\varnothing_1(k_f-k_{s1})}{k_{s1}+(m-1)k_f+\varnothing_1(k_f-k_{s1})}(k_f)=\frac{k_{s1}+2k_f-2\varnothing_1(k_f-k_{s1})}{k_{s1}+2k_f+\varnothing_1(k_f-k_{s1})}(k_f)$ m = 3(for spherical nanoparticle)	$k_{hnf}=\frac{k_{s2}+(m-1)k_{nf}-(m-1)\varnothing_2(k_{nf}-k_{s2})}{k_{s2}+(m-1)k_{nf}+\varnothing_2(k_{nf}-k_{s2})}(k_{nf})=\frac{k_{s2}+k_{nf}-2\varnothing_2(k_{nf}-k_{s2})}{k_{s2}+2k_{nf}+\varnothing_2(k_{nf}-k_{s2})}(k_{nf})$ m = 3(for spherical nanoparticle)
Electrical Conductivity	$\sigma_{nf}=\frac{(2\sigma_f+\sigma_{s1})+2\varnothing_1(\sigma_{s1}-\sigma_f)}{(2\sigma_f+\sigma_{s1})+\varnothing_1(\sigma_f-\sigma_{s1})}\cdot(\sigma_f)$	$\sigma_{hnf}=\frac{(\sigma_{s2}+2\sigma_{nf})-2\varnothing_2(\sigma_{nf}-\sigma_{s2})}{(\sigma_{s2}+2\sigma_{nf})+\varnothing_2(\sigma_{nf}-\sigma_{s2})}\times\frac{(\sigma_{s1}+2\sigma_f)-2\varnothing_1(\sigma_f-\sigma_{s1})}{(\sigma_{s1}+2\sigma_f)+\varnothing_1(\sigma_f-\sigma_{s1})}\cdot(\sigma_f)$

$$\left.\begin{aligned}\zeta = y\left(\frac{U}{2\upsilon_f x}\right)^{1/2},\ \psi = \left(2\upsilon_f xU\right)^{1/2} f(\zeta),\\ \theta(\zeta) = \frac{T-T_\infty}{T_w-T_\infty},\ \phi(\zeta) = \frac{C-C_\infty}{C_w-C_\infty}\\ u = Uf'(\zeta), v = \left(\frac{U\upsilon_f}{2x}\right)^{1/2}\left[\zeta f'(\zeta) - f(\zeta)\right]\end{aligned}\right\} \quad (6)$$

The variable viscosity Ahmed *et al.*,[5] is an inverse linear function of temperature and is denoted as:

$$\frac{1}{\mu} = \frac{1}{\mu_\infty}[1+\chi(T-T_\infty)] \quad (7)$$

where μ_∞ Is the dynamic viscosity at ambient temperature and

χ Is a thermal property of fluid.

The dimensionless form of temperature is

$$\theta = \frac{T-T_r}{T_w-T_\infty} + \theta_r \quad (8)$$

where $\theta_r = \frac{T_r-T_\infty}{T_w-T_\infty} = -\frac{1}{\chi(T_w-T_\infty)}$

Using the above parameter, the coefficient of viscosity for the hybrid nanofluid is

$$\mu_{hnf}(T) = \mu_{hnf}\left(\frac{\theta_r}{\theta_r-\theta}\right) \quad (9)$$

where θ_r stands for variable viscosity parameter

The variable thermal conductivity k is expressed as a function of temperature and as per Chaudhary *et al.*,[2] and Ahmed *et al.*,[5]:

$$K_{hnf}(T) = K_{hnf}(1+\varepsilon\theta) \quad (10)$$

with ε being a variable thermal conductivity parameter

The resulting non-linear ODE's on substituting Equation (6), (9), (10) into Equations (2), (3) and (4)

$$\left(\frac{\theta_r}{\theta_r-\theta}\right)f'''+\left(\frac{\theta_r}{(\theta_r-\theta)^2}\right)f''\theta' - A_4A_6M\ (f'-1) - \quad (11)$$

$$K(f'-1)+A_1(ff'')=0$$

$$(1+\varepsilon\theta)\theta''+\varepsilon\theta'^2+\frac{\Pr}{A_5}\left[\frac{A_6MEc}{A_4}\left(f'-1\right)^2+\frac{Ec}{A_4}f''^2\left(\frac{\theta_r}{\theta_r-\theta}\right)+Q\theta+A_3f\right] \quad (12)$$

$$\phi'' - ScC_r\phi + Scf\phi' = 0 \quad (13)$$

Transformed boundary conditions are as follows

$$\left.\begin{aligned}f(0)=S,\ f'(0)=\lambda+\sigma f''(0),\ \theta(0)=1,\ \phi(0)=1\ as\ \zeta=0,\\ f'(\zeta)\to 1,\ \theta(\zeta)\to 0,\ \phi(\zeta)\to 0\ as\ \zeta\to\infty\end{aligned}\right\} \quad (14)$$

Defined and associated parameters

$$\left.\begin{aligned}\text{K} = \text{porosity parameter} = \frac{\upsilon_f}{Uk^*},\\ \text{Pr} = \text{Prandtl number} = \frac{\upsilon_f(\rho Cp)_f}{k_f}\\ \text{M} = \text{Magnetic parameter} = \frac{B_0^2\sigma_f}{U\rho_f},\\ \text{Q} = \text{Heat source parameter} = \frac{Q_0}{U(\rho C_p)_f}\\ \text{Ec} = \text{Eckert Number} = \frac{U^2}{(T_w-T_\infty)(\rho C_p)_f},\\ \text{Sc} = \text{Schmidt number} = \frac{\upsilon_f}{D_m}\\ \text{C}_\text{r} = \text{Chemical Reaction Parameter} = \frac{k_r}{U}\end{aligned}\right\} \quad (15)$$

$$\left.\begin{aligned}A_1 = \left(\frac{\frac{\rho_{hnf}}{\rho_f}}{\frac{\mu_{hnf}}{\mu_f}}\right) = \left((1-\varnothing_2)\left[(1-\varnothing_1)+\varnothing_1\frac{\rho_{s1}}{\rho_f}\right]+\varnothing_2\frac{\rho_{s2}}{\rho_f}\right)\\ *\left((1-\varnothing_1)^{2.5}(1-\varnothing_2)^{2.5}\right)\\ A_2 = \left(\frac{\rho_{hnf}}{\rho_f}\right) = \left((1-\varnothing_2)\left[(1-\varnothing_1)+\varnothing_1\frac{\rho_{s1}}{\rho_f}\right]+\varnothing_2\frac{\rho_{s2}}{\rho_f}\right)\\ A_3 = \left(\frac{(\rho Cp)_{hnf}}{(\rho Cp)_f}\right) = \left((1-\varnothing_2)\left[(1-\varnothing_1)+\varnothing_1\frac{(\rho Cp)_{s1}}{(\rho Cp)_f}\right]+\varnothing_2\frac{(\rho Cp)_{s2}}{(\rho Cp)_f}\right)\\ A_4 = \left(\frac{\mu_f}{\mu_{hnf}}\right) = \left((1-\varnothing_1)^{2.5}(1-\varnothing_2)^{2.5}\right)\\ A_5 = \frac{k_{hnf}}{k_f} = \left(\frac{\left(\frac{\varnothing_1k_{s1}+\varnothing_2k_{s2}}{\varnothing_1+\varnothing_2}\right)+2k_f+2(\varnothing_1k_{s1}+\varnothing_2k_{s2})-2(\varnothing_1+\varnothing_2)k_f}{\left(\frac{\varnothing_1k_{s1}+\varnothing_2k_{s2}}{\varnothing_1+\varnothing_2}\right)+2k_f-(\varnothing_1k_{s1}+\varnothing_2k_{s2})+(\varnothing_1+\varnothing_2)k_f}\right)\\ A_6 = \frac{\sigma_{hnf}}{\sigma_f} = \left(\frac{\sigma_{s2}(1+2\varnothing_2)+2\sigma_f(1-\varnothing_2)}{\sigma_{s2}(1-\varnothing_2)+\sigma_f(2+\varnothing_2)}\right)*\frac{\sigma_{s1}(1+2\varnothing_1)+2\sigma_f(1-\varnothing_1)}{\sigma_{s1}(1-\varnothing_1)+\sigma_f(2+\varnothing_1)}\end{aligned}\right\} \quad (16)$$

2.2 Mathematical Expressions for Quantities of Interest

Skin friction coefficient Cf_x, Nusselt number Nu_x, and Sherwood number Sh_x are defined as

$$Cf_x = \frac{\tau_w}{\rho_f u_w^2},\ Nu_x = \frac{xq_w}{k_f\left(T_w - T_\infty\right)},\ Sh_x = \frac{xq_m}{D_B\left(C_w - C_\infty\right)}$$

$$\tau_w = \mu_{hnf}(T)\left(\frac{\partial u}{\partial y}\right)_{y=0},\ q_w = -k_{hnf}\left(T\right)\left(\frac{\partial T}{\partial y}\right)_{y=0},$$

$$q_m = -D_B\left(\frac{\partial C}{\partial y}\right)_{y=0},\ \tau_w = \mu_{hnf}\left(\frac{\theta_r}{\theta_r - \theta}\right)\left(\frac{\partial u}{\partial y}\right)_{y=0}, \tag{17}$$

$$q_w = -k_{hnf}\left(1+\varepsilon\theta\right)\left(\frac{\partial T}{\partial y}\right)_{y=0},$$

$$Nu_x = -\frac{x}{k_f\left(T_f - T_\infty\right)}\left[k_{hnf}\left(1+\varepsilon\theta\right)\left(\frac{\partial T}{\partial y}\right)_{y=0}\right]$$

$$Re_x^{1/2} f_x = \left(\frac{\theta_r}{\theta_r - \theta}\right)\left(\frac{f''(0)}{\sqrt{2A_4}}\right)$$

$$Re_x^{-1/2} Nu_x = -\frac{A_5}{\sqrt{2}}\left(1+\varepsilon\theta\right)\theta'(0) \tag{18}$$

$$Re_x^{-1/2} Sh_x = -\frac{\phi'(0)}{\sqrt{2}} \tag{19}$$

where Re_x is the local Reynolds' number given by $Re_x = \frac{Ux}{\upsilon_f}$

3.0 Numerical Procedure

An effective numerical approach with precise convergence must be employed for the system of equations. The numerical results are derived using the bvp4c method in MATLAB. In comparison to alternative numerical methods, the bvp4c technique is more versatile and facilitates enhanced precision in controlling approach criteria. The subsequent elements of the computing framework are as follows:

Using appropriate substitution as below,

$f(\zeta) = y(1)$ $\quad f'(\zeta) = y(2)$ $\quad f''(\zeta) = y(3)$
$\theta(\zeta) = y(4)$ $\quad \theta'(\zeta) = y(5)$ $\quad \phi(\zeta) = y(6)$ $\quad \phi'(\zeta) = y(7)$

The first-order system of equations obtained is

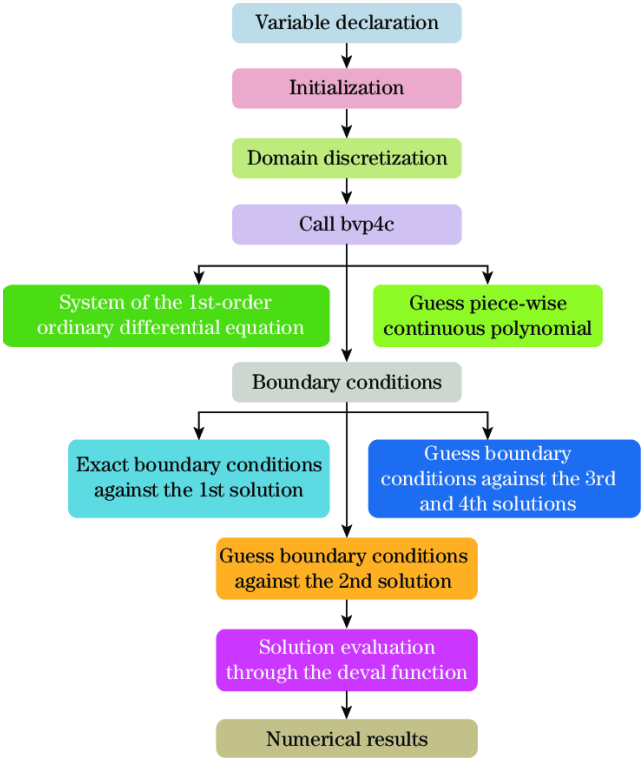


Figure 2. Steps of numerical solutions.

$$\begin{bmatrix} y(1)\\ y(2)\\ y(3)\\ y(4)\\ y(5)\\ y(6)\\ y(7) \end{bmatrix} = \begin{bmatrix} y(2)\\ y(3)\\ \left(\frac{\theta_r - y(4)}{\theta_r}\right)*\begin{pmatrix} K*\left(y(2)-1\right)+A_4*A_6*M\\ *\left(y(2)-1\right)-A_1*y(1)*y(3)\\ -\left(\frac{\theta_r}{(\theta_r-\theta)^2}\right)*y(3)*y(5) \end{pmatrix}\\ y(5)\\ -\frac{1}{1+\varepsilon y(4)}\begin{pmatrix} \varepsilon y(5)^2+\left(\frac{Pr}{A_5}\right)\\ *\begin{pmatrix} A_6*M*Ec*\left(y(2)-1\right)^2\\ +\frac{Ec}{A_4}*y(3)^2\left(\frac{\theta_r}{\theta_r-y(4)}\right)\\ +Q*y(4)+A_3*y(1)*y(5) \end{pmatrix} \end{pmatrix}\\ y(7)\\ Sc*\left(C_r*y(6)-y(1)*y(7)\right) \end{bmatrix}$$

The revised initial boundary conditions are specified as follows:

$$\begin{bmatrix} y_a(1) \\ y_a(2) \\ y_a(5) \\ y_a(7) \\ y_b(2) \\ y_b(4) \\ y_b(6) \end{bmatrix} = \begin{bmatrix} y_a(1)-S \\ y_a(2)-\text{»}-\sigma_L y_a(3) \\ y_a(4)-1 \\ y_a(6)-1 \\ y_b(2)-1 \\ y_b(4) \\ y_b(6) \end{bmatrix}$$

4.0 Results and Discussions

Starting assumptions, boundary layer thickness and other parameters must be calibrated in the coding function for accurate results. We calculate the impact of different factors on the SWCNT-MWCNT hybrid nanofluid with water. Numerical computations are conducted for various values of the parameters such as θ_r, ε,λ, *Ec, Cr, Sc, Q and* σ_L aiming to provide a comprehensive insight into the problem. The parameter ranges are defined as follows: $\theta_r(1.2 \le \theta_r \le 1.8)$, $\varepsilon(0.2 \le \varepsilon \le 0.8)$, $\lambda(0.2 \le \lambda \le 0.8)$, $Ec(0.01 \le Ec \le 0.07)$, $Cr(0.1 \le Cr \le 0.7)$, $Sc(0.62 \le Sc \le 0.92)$, $Q(0.2 \le Q \le 0.5)$, σ_L $(0 \le \sigma_L \le 0.6)$. The Prandtl number and nanoparticle volume fraction for SWCNT, MWCNT will remain at Pr = 6.2 and $\varphi_1 = \varphi_2 = 0.01$ in the study. To determine how moving plate, Eckert number, velocity slip, heat source, Schmidt number, and chemical reaction parameters impact mass, heat transfer, boundary layer flow with viscosity, thermal conductivity, they will be tested. Findings are tabulated.

Figures 3 and 4 display values of $Re_x^{1/2} C_f$ and $Re_x^{-1/2} Nu_x$ with λ at changes in θ_r and ε when Pr = 6.2, $\varphi_1 = 0.01$, $\varphi_2 = 0.02$, M = Q = Ec = 0.01, Sc = 0.62, Cr = K = σ_L = 0.5 for SWCNT-MWCNT/water.

When a moving plate approaches or recedes, viscosity dynamics, Reynolds number, and heat impact the skin friction coefficient. Figure 3 shows that increasing fluid viscosity increases skin friction and drag when moving surfaces towards and away from an origin. Fluid swirling while a plate moves thins the thermal barrier layer and increases heat transfer. Figure 4 indicates that lowering boundary layer thickness increases the Nusselt number and heat transfer coefficient.

Figure 5 shows that augmented slip reduces skin friction for a plate moving towards the origin and wall shear stress for a plate moving away from the origin by lowering the velocity gradient at the wall. Increased slip reduces the Nusselt number for a plate moving in the origin because it lowers heat transfer efficiency. The Nusselt number decreases further when the slip ratio is raised for the plate moving away from the origin in Picture 6.

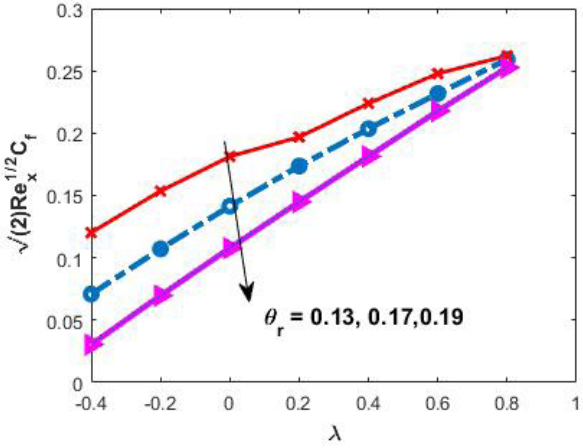


Figure 3. Distribution of skin friction coefficient with variations in θ_r and λ.

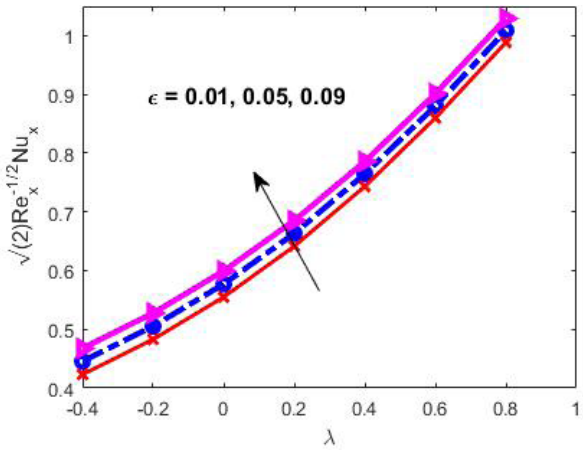


Figure 4. Distribution of heat transfer coefficient with variations in ε and λ.

Figure 7 shows velocity profiles increasing with varying viscosity parameter in hybrid nanofluids (SWCNT + MWCNT in water). In natural convection and high-shear situations, these characteristics lower flow resistance and increase velocity.

Changing the viscosity parameter θ_r decreases temperature and concentration profiles by increasing convective heat transfer (Figures 8 and 9). Velocity increases convective heat transfer, lowering temperature. High viscosity stabilises flow and inhibits nanoparticle clumping, enhancing mass diffusion. Mixing quicker and lowering the concentration lowers the concentration profile.

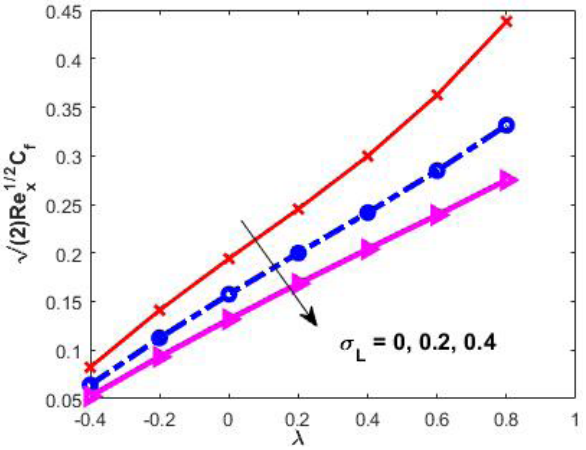


Figure 5. Distribution of skin friction coefficient with variations in σ_L and λ.

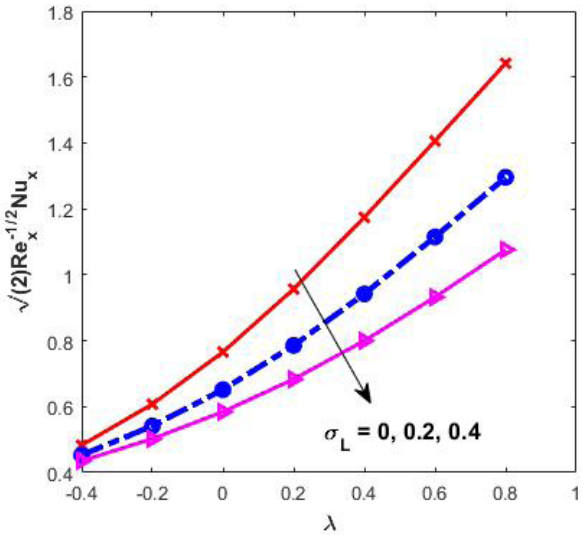


Figure 6. Distribution of heat transfer coefficient with variations in σ_L and λ.

High thermal conductivity ε facilitates fluid heat transport. A hybrid nanofluid (SWCNT + MWCNT with water) reduces temperature gradients and buoyancy forces, decreasing the velocity profile in Figure 10.

Nanofluids with higher thermal conductivity transfer heat faster. Fluid concentrations rise as nanoparticles collect. Figures 11 and 12 illustrate that larger concentration and heat boundary layers impair transport efficiency, raising profiles. As can be seen in Figure 13, increase in slip parameter σ_L causes higher velocity profiles in hybrid nanofluid. A decrease in thermal resistance results in a decrease in temperature profiles because heat is able to disperse more effectively, as may be seen in picture 14.

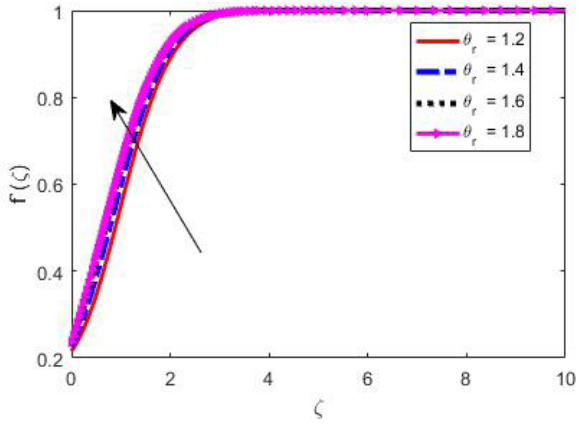


Figure 7. θ_r effects on velocity profiles.

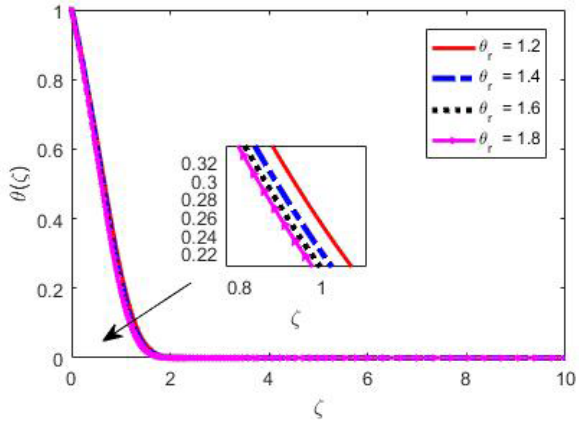


Figure 8. θ_r effects on temperature profiles.

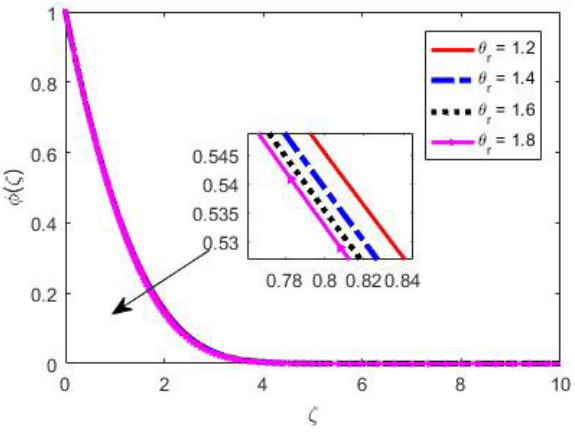


Figure 9. θ_r effects on concentration profiles.

Fluid layers are stretched along with the moving plate parameter λ as it moves away from the origin, which results in an increase in velocity during the moving plate, as shown in Figure 15. Nanoparticles promote heat

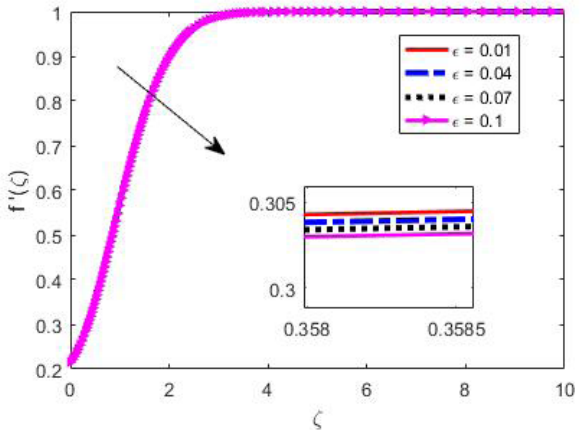


Figure 10. ε effects on velocity profiles.

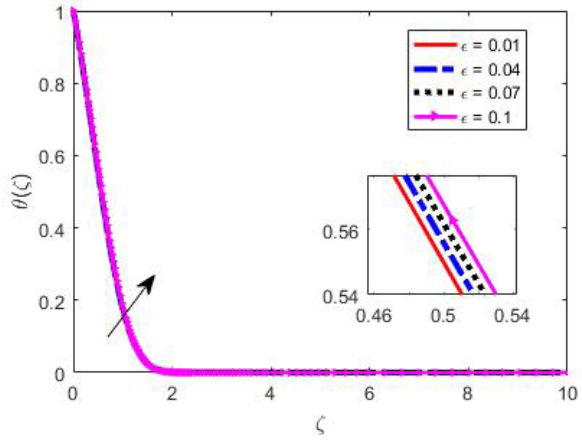


Figure 11. ε effects on temperature profiles.

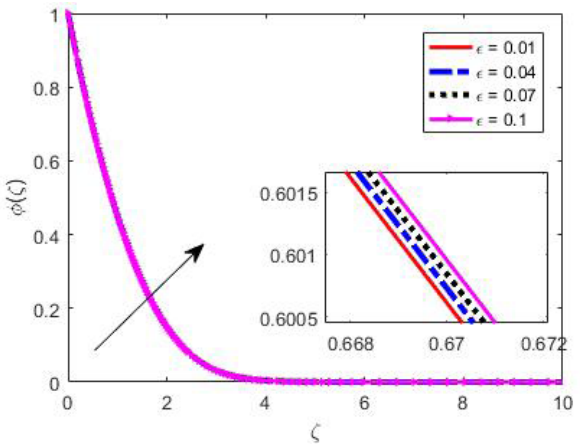


Figure 12. ε effects on concentration profiles.

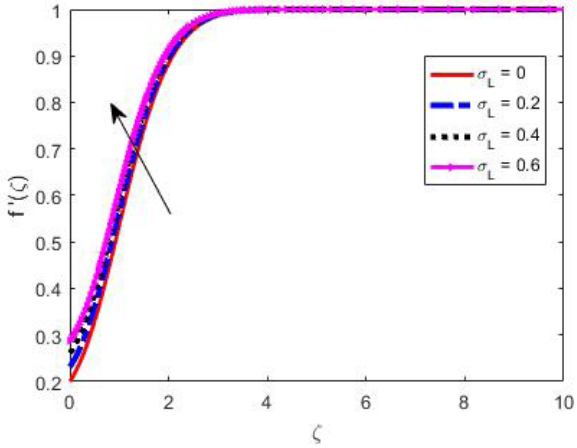


Figure 13. σ_L effects on velocity profiles.

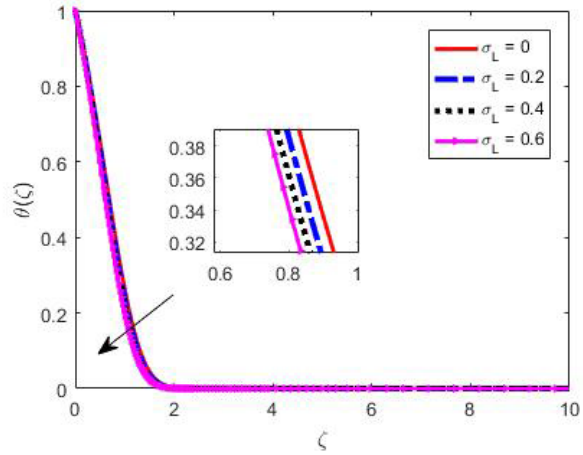


Figure 14. σ_L effects on temperature profiles.

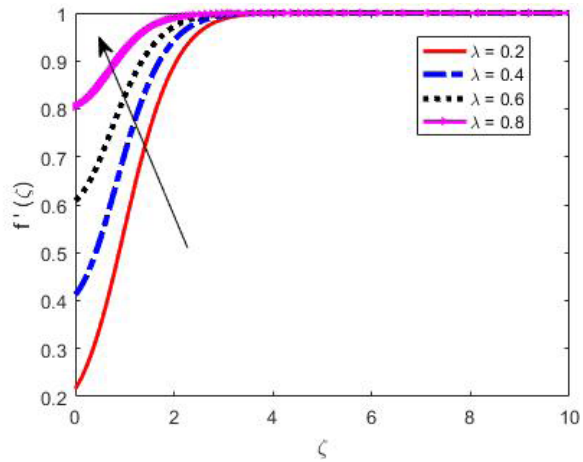


Figure 15. λ effects on velocity profiles.

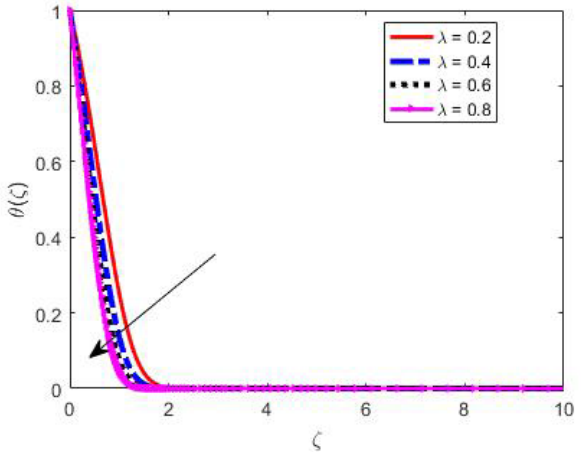


Figure 16. λ effects on temperature profiles.

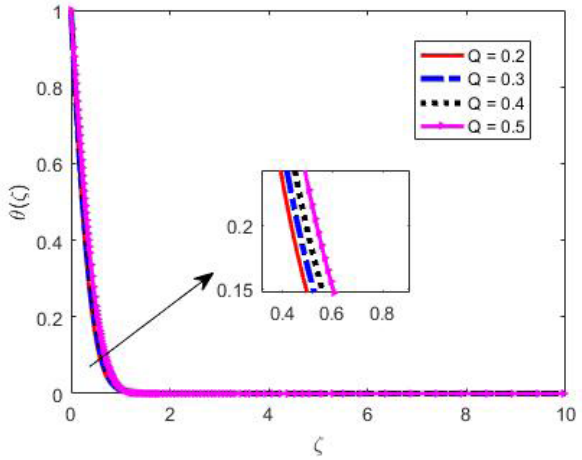


Figure 18. Q effects on temperature profiles

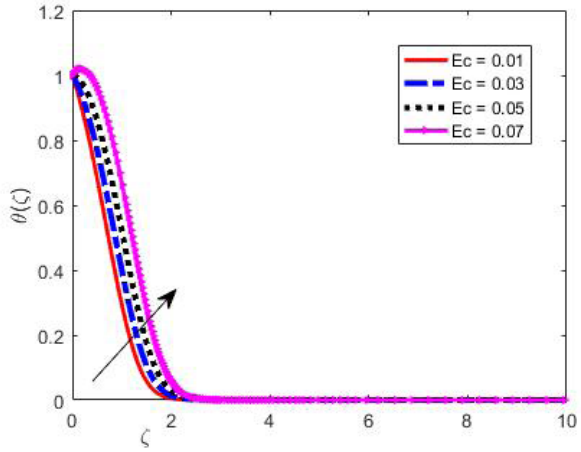


Figure 17. Ec effects temperature profiles

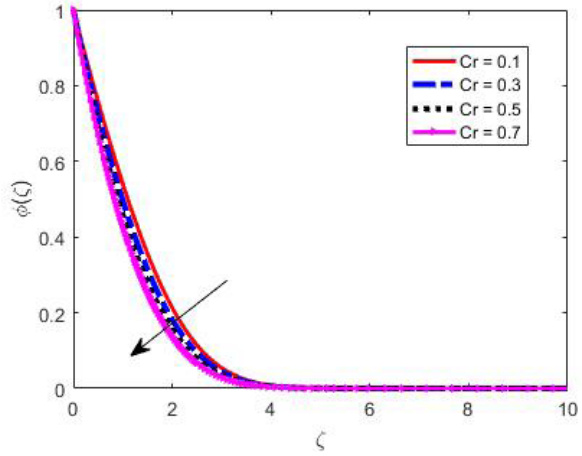


Figure 19. Cr effects on concentration profiles.

conduction, which in turn allows heat to disperse more quickly, this results in temperature profiles that are lower, as displayed in Figure 16. Figure 17 illustrates a rise in the temperature profile. An elevated Eckert number (Ec) indicates intensified viscous dissipation, resulting in an elevated temperature profile due to increased heat retention in the boundary layer. A heat source Q in a hybrid nanofluid provides supplementary thermal energy to the fluid with an increase in temperature profile, as in Figure 18.

The concentration profile in a hybrid nanofluid (SWCNT + MWCNT with water as the base fluid) is influenced by the chemical reaction Cr and the Schmidt number Sc, which impact mass transfer and species diffusion, as seen in Figures 19 and 20. The concentration profile diminishes as the reactant species are exhausted.

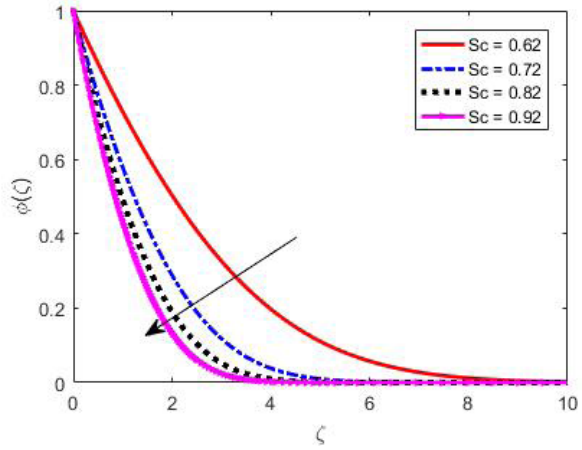


Figure 20. Sc effects on concentration profiles.

Table 3. Variations in $Re_x^{1/2} C_{fx}$ (skin friction coefficient) and $Re_x^{-1/2} Nu_x$ (Nusselt number)

M	K	θ_r	ε	Ec	$Re_x^{1/2} C_{fx}$	$Re_x^{-1/2} Nu_x$
0.01	0.5	0.18	0.01	0.05	0.57958	1.33042
0.05					0.57981	1.32522
0.1					0.58281	1.28118
0.5	0.1				0.54305	1.24359
	0.3				0.56469	1.00163
	0.5				0.64053	0.92710
	0.1	0.1			0.22066	1.20041
		0.13			0.34434	1.31005
		0.15			0.42892	1.32637
		0.18	0.01		0.54305	1.24359
			0.04		0.54032	1.26190
			0.1		0.53268	1.29062
			0.01	0.01	0.58112	1.05620
				0.03	0.56169	1.15951
				0.05	0.54305	1.24359

Table 4. Influence of φ_2, Sc and Cron - φ'(0)

φ_2	Sc	Cr	- φ'(0)
0.02	0.4	0.2	0.360326491
0.03			0.361487218
0.05			0.363912246
0.02	0.5		0.398365572
	0.6		0.433350659
	0.7		0.466091261
	0.4	0.3	0.408487471
		0.4	0.452745864
		0.5	0.493806594

An elevated Schmidt number indicates reduced mass diffusivity, signifying that the species diffuse more slowly into the nanofluid.

Table 3 shows that the skin-friction coefficient increases with higher M, K, and θ_r, and decreases with higher ε and Ec. It also indicates that the Nusselt number decreases with higher M,K., but increases with an increase in θ_r, ε and Ec. Table 4 reveals that the mass transfer coefficient increases with φ_2, Sc and Cr. These findings highlight the varying impacts of different parameters on friction, heat, and mass transfer in engineering contexts.

A validation is performed by comparing the computed values of the skin friction coefficient –f''(0) with existing results available in the literature. Specifically, Table 5 presents a comparison for selected values of the parameters ϕ_1, ϕ_2, and λ using benchmark results reported by Aladdin *et al.,*[12] and Khan *et al*[13]. The good agreement observed between the present results and those in prior studies confirms the validity of the adopted numerical approach.

Table 5. Comparison of skin friction f''(0) when M = S = Ec = σ_L = Sc = Cr = Q = 0

φ_1	φ_2	λ	Khan[13] *et al*	Aladdin[12] *et al*	Present Results
0	0	0	0.4696	0.4696	0.4696
0	0.01	-0.25	-	0.3977	0.3977
		-0.15	-	0.4448	0.4447
		0	-	0.4651	0.4649
		0.2	-	0.4389	0.4387
0.01	0.01	-0.25	-	0.3958	0.3956
		-0.15	-	0.4426	0.4427
		0	-	0.4629	0.4627
		0.2	-	0.4369	0.4368

5.0 Conclusions

(i) As the plate travels away from the origin, an increase in variable viscosity results in a drop in the

skin friction coefficient, whilst an increase in heat conductivity elevates the Nusselt number.

(ii) An increase in the slip parameter reduces both skin friction and the Nusselt number as the plate travels away from the origin.

(iii) An increase in variable viscosity elevates the velocity while diminishing temperature and concentration profiles.

(iv) Velocity patterns diminish, whereas temperature and concentration profiles augment with an increase in variable thermal conductivity.

(v) An increase in the slip parameter elevates velocity profiles while reducing temperature.

(vi) As the plate recedes from the origin, velocity profiles grow while temperature profiles drop.

(vii) Temperature profiles grow with both the Eckert number and the heat source.

(viii) An increase in Schmidt number and chemical reactions diminishes concentration profiles.

6.0 Funding

The authors thank SAGTE for their encouragement and financial support.

7.0 Authors' Contributions

Conceptualisation, methodology, validation of results investigation and supervision by J.L. Rama Prasad. Formal analysis, investigation and original draft preparation by K. Fatima. All authors have read and agreed to the published version of the manuscript.

8.0 References

1. AbuBakar S, Arifin NM, Pop I. Mixed convection hybrid nanofluid flow past a stagnation-point region with variable viscosity and second-order slip. J Adv Res Micro Nano Eng. 2023; 12(1):1-21. https://doi.org/10.37934/armne.12.1.121
2. Chaudhary H, Sunil D, Mishra VN. Effects of variable viscosity and thermal conductivity on MHD flow due to the permeable moving plate. Stoch Model Appl. 2021; 25(2):271-288.
3. Fusi L, Tozzi R. Falkner-Skan boundary layer flow of a fluid with pressure-dependent viscosity past a stretching wedge with suction or injection. Int J Non Linear Mech. 2024; 163:104746. https://doi.org/10.1016/j.ijnonlinmec.2024.104746
4. Manjunatha S, Kuttan BA, Jayanthi S, Chamkha A, Gireesha BJ. Heat transfer enhancement in the boundary layer flow on hybrid nanofluids due to variable viscosity and natural convection. Heliyon. 2019; 5(4):e01469. https://doi.org/10.1016/j.heliyon.2019.e01469 PMid:30997430 PMCid:PMC6451174
5. Ahmad S, Nadeem S, Ullah N. Entropy generation and temperature-dependent viscosity in the study of SWCNT-MWCNT hybrid nanofluid. Appl Nanosci. 2020. https://doi.org/10.1007/s13204-020-01306-0
6. Abdal S, Fatmawati, Chukwu CW. Significance of variable viscosity for time-dependent flow of hybrid nanofluids due to spinning surface. Alexandria Eng J. 2023; 71:551-563. https://doi.org/10.1016/j.aej.2023.03.051
7. Dharmaiah G, Chamkha A, Vedavathi N, Balamurugan KS. Viscous dissipation effect on transient aligned magnetic free convective flow past an inclined moving plate. Front Heat Mass Transf. 2019; 12(17):1-11. https://doi.org/10.5098/hmt.12.17
8. Vedavathi N, Dharmaiah G, Abdul Gaffar S, Venkatadri K. Entropy analysis of nanofluid magnetohydrodynamic convection flow past an inclined surface: A numerical review. Heat Transf. 2021. https://doi.org/10.1002/htj.22159
9. Zeeshan A, Shehzad N, Atif M, Ellahi R, Sait SM. Electromagnetic flow of SWCNT/MWCNT suspensions in two immiscible water- and engine-oil-based Newtonian fluids through porous media. Symmetry. 2022; 14:406. https://doi.org/10.3390/sym14020406
10. Murtaza S, Kumam P, Bilal M, Sutthibutpong T, Rujisamphan N, Ahmed Z. Parametric simulation of hybrid nanofluid flow consisting of cobalt ferrite nanoparticles with second-order slip and variable viscosity over an extending surface. Nanotechnol Rev. 2023; 12:20220533. https://doi.org/10.1515/ntrev-2022-0533
11. Hanif H, Jamshed W, Devi SSU, Eid MR, Shafie S, Ibrahim RW. Thermal description and entropy evaluation of magnetized hybrid nanofluid with variable viscosity via Crank-Nicolson method. Case Stud Therm Eng. 2023; 47:103132. https://doi.org/10.1016/j.csite.2023.103132
12. Aladdin NA, Anuar NS, Bachok N, Ali F. Effects of Joule heating and slip on magnetohydrodynamics hybrid carbon nanotubes flow through a permeable moving plate. J Adv Res Micro Nano Eng. 2024; 24(1):52-66. https://doi.org/10.37934/armne.24.1.5266
13. Khan WA, Culham R, Ul Haq R. Heat transfer analysis of MHD water functionalized carbon nanotube flow over a static/moving wedge. J Nanomater. 2015. https://doi.org/10.1155/2015/934367

14. Konwar H. Flow, heat and mass transfer past a stretching sheet with temperature-dependent fluid properties in porous medium. J Heat Mass Transf Res. 2022; 9:17-26.
15. Lakshmi BN, Dharmaiah G, Anjum A, Samdani, Naheed M. Influence of Darcy-Forchheimer Fe_3O_4-$CoFe_2O_4$-H_2O hybrid nanofluid flow with magnetohydrodynamic and viscous dissipation effects past a permeable stretching sheet: a numerical contribution. Multiscale Multidiscip Model Exp Des. 2025; 8:115. https://doi.org/10.1007/s41939-024-00694-y
16. Goud BS, Dharmaiah G. Role of Joule heating and activation energy on MHD heat and mass transfer flow in the presence of thermal radiation. Numer Heat Transf B. 2023; 84(5):620-641. https://doi.org/10.1080/10407790.2023.2215917
17. Isaac Lare A. Casson fluid flow with variable viscosity and thermal conductivity along exponentially stretching sheet embedded in a thermally stratified medium with exponentially heat generation. J Heat Mass Transf Res. 2015; 2:63-78.
18. Reddy BN, Poornima T, Sreenivasulu P. Influence of variable thermal conductivity on MHD boundary layer slip flow of ethylene-glycol based Cu nanofluids over a stretching sheet with convective boundary condition. Int J Eng Math. 2014. https://doi.org/10.1155/2014/905158
19. Ganga B, Charles S, Abdul Hakeem AK, Nayak MK, Muhammad T, Albogami N, Sivasankaran S. Numerical treatment for 3D magnetized Casson fluid flow over an unsteady convectively heated surface with variable thermal conductivity. Therm Sci. 2023; 27(1A):359-373. https://doi.org/10.2298/TSCI210611174G
20. Sreenivasulu P, Poornima T, Reddy BN. Variable thermal conductivity influence on hydromagnetic flow past a stretching cylinder in a thermally stratified medium with heat source/sink. Front Heat Mass Transf. 2017; 9(20). https://doi.org/10.5098/hmt.9.20
21. Babar H, Sajid MU, Ali HM. Viscosity of hybrid nanofluids: A critical review. Therm Sci. 2019; 23(3B):1713-1754. https://doi.org/10.2298/TSCI181128015B
22. Alarabi TH, Mahdy A. Variable thermal conductivity and thermophoretic aspects of free convection flow of a micropolar fluid due to a permeable cone with heat source/sink. AIP Adv. 2022; 12:095308. https://doi.org/10.1063/5.0106500
23. Sharma VK, Rafi A. Effect of variable thermal conductivity and heat source/sink near a stagnation point on a linearly stretching sheet using HPM. Glob J Sci Front Res F Math Decis Sci. 2014; 14(2).
24. Singh V, Agarwal S. MHD flow and heat transfer for Maxwell fluid over an exponentially stretching sheet with variable thermal conductivity in porous medium. Therm Sci. 2014; 18(2):S599-S615. https://doi.org/10.2298/TSCI120530120S

Nomenclature

U	Characteristic velocity of the moving plate(m/s)
f (ζ)	dimensionless stream function)
τ_w	W all shear stress (kg/ms^2)
k	Thermal conductivity of the fluid(W/mK)
ρ	Density of the fluid (kg/m^3)
C_p	Specific heat at constant pressure(J/kgK)
ρC_p	Heat capacitance of fluid (J/Km^3)
α	Thermal diffusivity(m^2/s)
σ	Electrical conductivity(S/m)
μ	Dynamic viscosity of the fluid (kg/ms)
T_w	Plate temperature (K)
T_∞	Ambient temperature (K)
C_w	Plate concentration(kg/m^3)
C_∞	Ambient concentration(kg/m^3)
ζ	Similarity variable
M	Magnetic field parameter
θ_r	Variable viscosity parameter
ε	VariableThermal conductivity parameter
Pr	Prandtl number
Ec	Eckert number
K	Porosity parameter
S	Suction
Sc	Schmidt number
Cr	Chemical reaction parameter
Q	Heat source parameter
σ_L	Slip parameter
λ	Moving ratio parameter
υ_f	kinematic viscosity of the fluid (m^2/s)
Nu_x	Nusselt Number
Re_x	Reynolds number
C_{fx}	Skin friction coefficient
φ_1	Nanoparticle concentration of SWCNT
φ_2	Nanoparticle concentration of SWCNT